



## MOTIVATION

- Climate change – increase frequency & severity of droughts & floods - necessitates innovative & reliable techniques for continuous monitoring of discharge to effectively manage risk.
- Objective:** Develop a data-driven river discharge estimation algorithm that generalizes well across diverse basins with varying hydroclimatic conditions.
- We utilized remotely-sensed water area, water indices, band values from optical, SAR, and altimetry satellites, in-situ discharge observations collected during field campaigns, and both machine learning (e.g., Random Forest Regression (RFR) (Breiman, 2001)) and deep learning method (e.g., Long-Short Term Memory (LSTM) (Hochreiter, S., & Schmidhuber, J., 1997) to estimate river discharge.

## DATASETS & PLATFORM

### Initial Approach:

- Google Earth Engine (GEE):** A powerful cloud-based spatial analysis platform providing publicly available satellite data in Javascript and Python language, without downloading images.
- Remotely-Sensed (RS) Data Sources:**
  - Sentinel-1 Synthetic Aperture Radar (SAR):** Water indices and backscatter bands extracted via GEE
  - Sentinel-2 Multispectral Images (Level-1C):** Water indices and reflectance bands extracted via GEE
- Ground Truth Discharge Measurements:**
  - The US Geological Survey (USGS, 2024) - Mississippi River
  - The Regional Agency for Environmental Protection - Po River
  - State Hydraulic Works of Türkiye (DSİ - Devlet Su İşleri, 2024) - Kizilirmak River
- Ongoing Work:**
  - Altimetry Data:** Sentinel-3 and Sentinel-6 from Hydroweb-next platform.
  - GLO-30 DEM:** Elevation & Slope features extracted via GEE
  - Seasonality Indicators:** sine/cos transformations (day-of-year) & monthly cycle

## SITE SELECTION

Study areas were selected based on their representation of diverse hydrological flow regimes. To support the development of a generalized and transferable river discharge estimation model, one area was chosen from each of three different basins: Memphis along the Mississippi River (USA), Pontelagoscuro along the Po River (Italy), and the Sogutluhan along Kizilirmak River (Türkiye) (Figure 1).

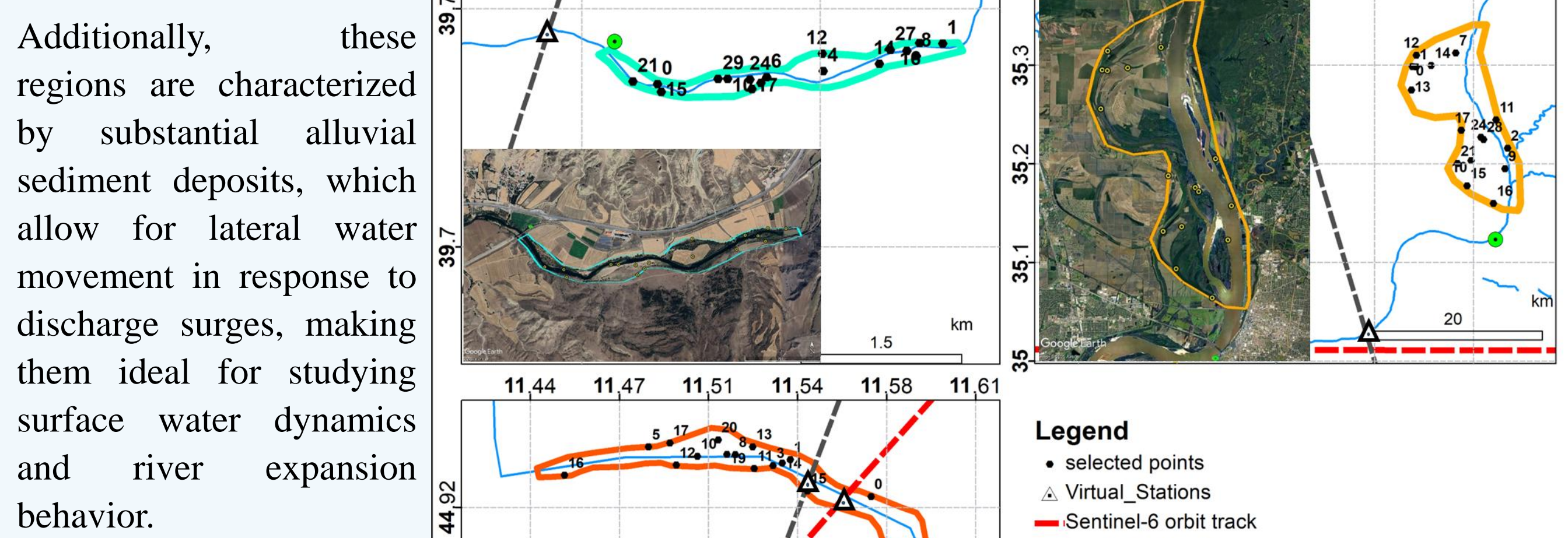


Figure 1: The geographic locations of study areas

## INITIAL APPROACH: RF MODELING

**Model Development:** The RFR model was initially trained and validated using 5-fold cross-validation. To evaluate temporal generalizability, the same model was later trained using a time-based split. The overall workflow is illustrated in Figure 2, while the performance results and visualized results across all study regions are presented in Table 1 and Figure 3, respectively.

In Table 1, RMSE and logRMSE are complementary: RMSE emphasizes flood dynamics, logRMSE captures low-flow reliability. R<sup>2</sup> presents the overall model fit.

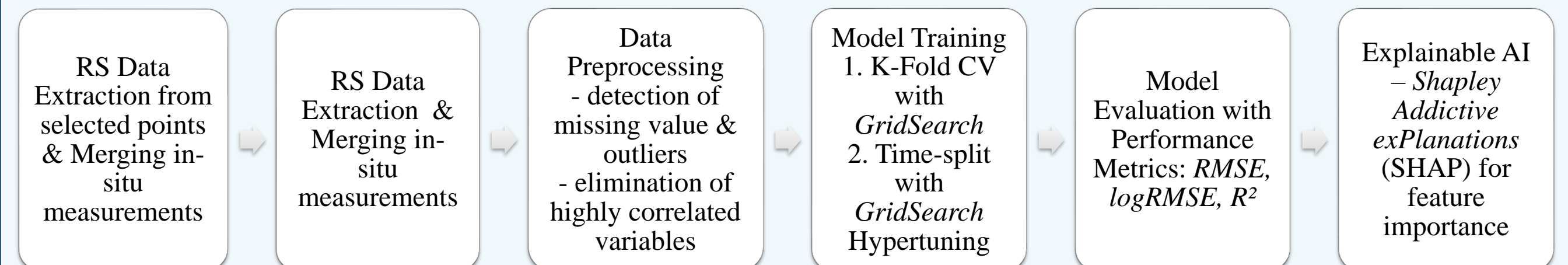


Figure 2: The RFR workflow for river discharge estimation with two different models

## REFERENCES

Breiman, L. (2001) Random Forests. Machine Learning, 45, 5-32. <https://dx.doi.org/10.1023/A:1010933404324>  
 Long short-term memory. Neural Computation, 9(8), 1735-1780. <https://doi.org/10.1162/neco.1997.9.8.1735>  
 European Space Agency. (2024). Sentinel-1. Retrieved from <https://sentinel.esa.int/web/sentinel/missions/sentinel-1>  
 European Space Agency. (2024). Sentinel-2. Retrieved from <https://sentinel.esa.int/web/sentinel/missions/sentinel-2>  
 Google Earth Engine. (2024). About Earth Engine. Retrieved from <https://developers.google.com/earth-engine>  
 Hochreiter, S., & Schmidhuber, J. (1997). Long short-term memory. Neural Computation, 9(8), 1735-1780.  
 Lundberg, S. M., & Lee, S.-I. (2017). A unified approach to interpreting model predictions. Advances in Neural Information Processing Systems (NeurIPS), 30.  
 U.S. Geological Survey, 2024, Earthquake Lists, Maps, and Statistics, accessed Mar 30, 2024 at URL <https://waterdata.usgs.gov/nwis/measurements>

## INITIAL APPROACH: RESULTS

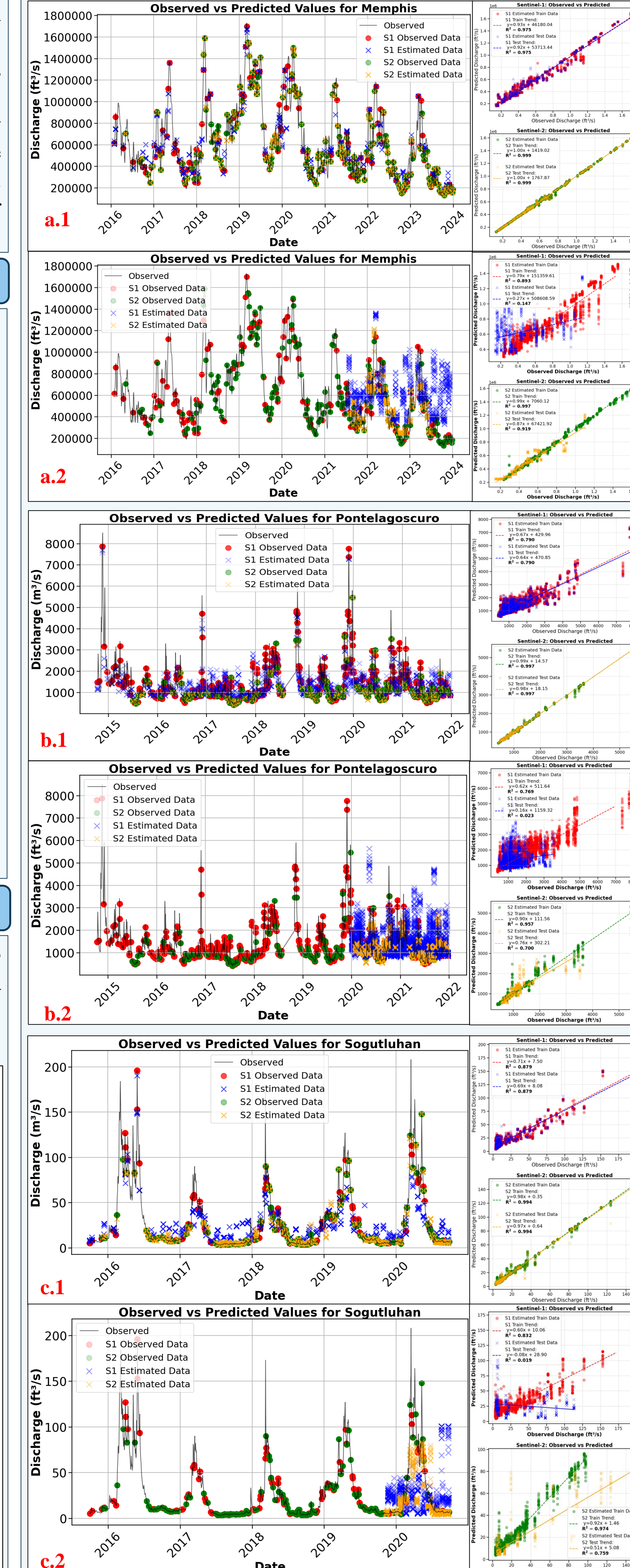


Figure 3: The results of the RFR model across all regions; (a.1) Memphis K-Fold CV, (a.2) Memphis Time-split, (b.1) Pontelagoscuro K-Fold CV, (b.2) Pontelagoscuro Time-split, (c.1) Sogutluhan K-Fold CV, (c.2) Sogutluhan Time-split

**Table 1:** The performance metrics of K-Fold CV and Time-split models across all proposed areas

| Study Site     | Memphis             |            | Pontelagoscuro      |            | Sogutluhan          |            |
|----------------|---------------------|------------|---------------------|------------|---------------------|------------|
|                | Performance Metrics | Time-split | Performance Metrics | Time-split | Performance Metrics | Time-split |
| RMSE           | 67532.64            | 311984.66  | 456.16              | 749.82     | 12.65               | 40.62      |
| logRMSE        | 0.15                | 0.72       | 0.30                | 0.47       | 0.59                | 1.35       |
| R <sup>2</sup> | 0.975               | 0.147      | 0.790               | 0.023      | 0.879               | 0.019      |
| RMSE           | 12401.09            | 249685.71  | 49.39               | 280.76     | 3.36                | 24.53      |
| logRMSE        | 0.02                | 0.15       | 0.18                | 0.53       | 0.94                | 0.759      |
| R <sup>2</sup> | 0.999               | 0.919      | 0.994               | 0.019      | 0.994               | 0.019      |

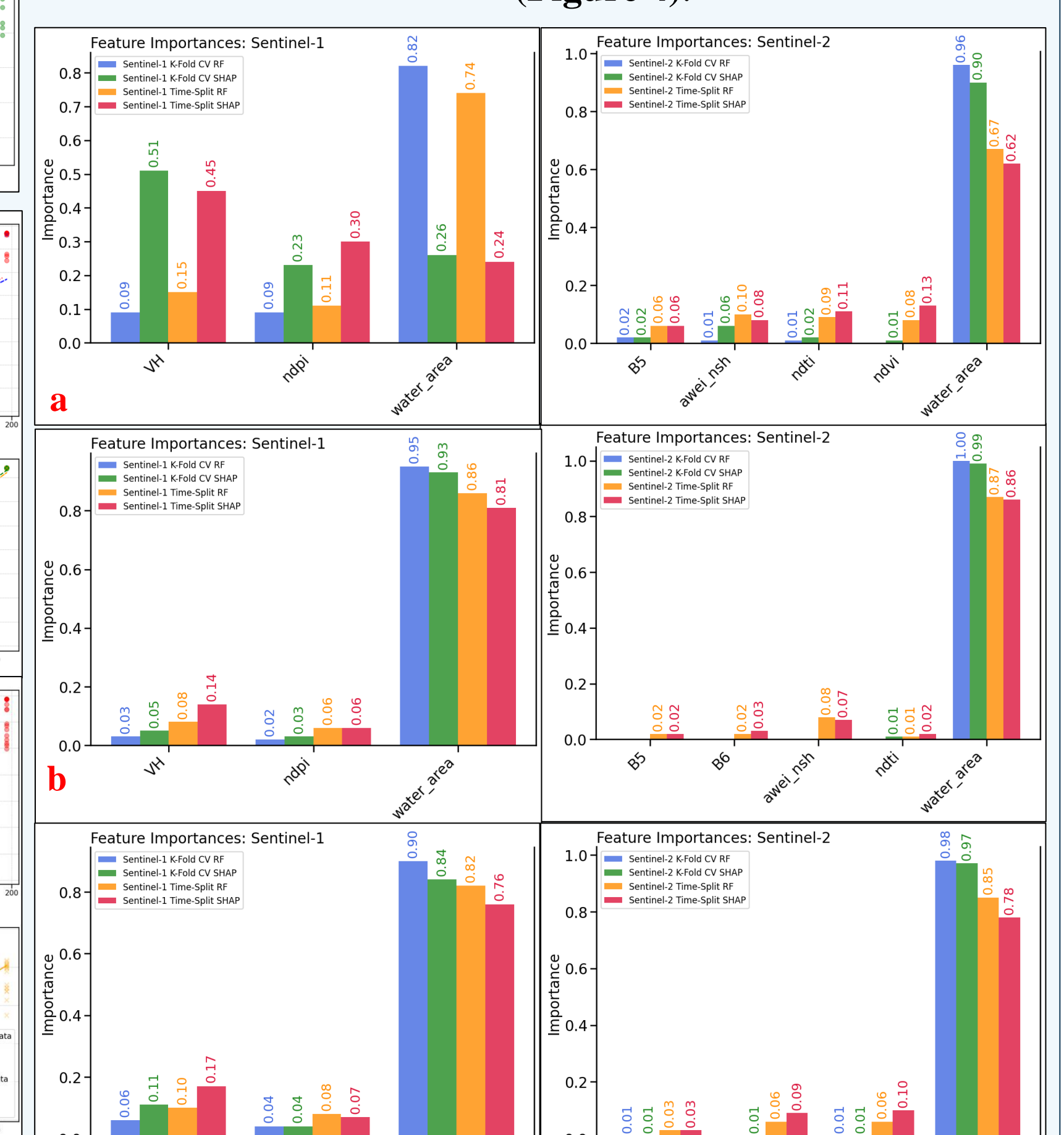


Figure 4: SHAP feature importance evaluation for both models across all areas; (a) Memphis, (b) Pontelagoscuro, and (c) Sogutluhan

## ADVANCED APPROACH: PRELIMINARY RESULTS

This section presents preliminary results of the time-aware LSTM model applied across all regions (Figure 6) using two distinct input configurations (Dataset 1: satellite-based data with Sentinel-1, altimetry water level, auxiliary data with ground-truth measurement; Dataset 2: satellite-based data with Sentinel-2, altimetry water level, auxiliary data with ground measurement). Additionally, scatter plots along full time-series of final results (Fold 5) illustrate the agreement between observed and predicted discharge values for both datasets with metric score evaluation in Figure 7 with the preliminary metric results.

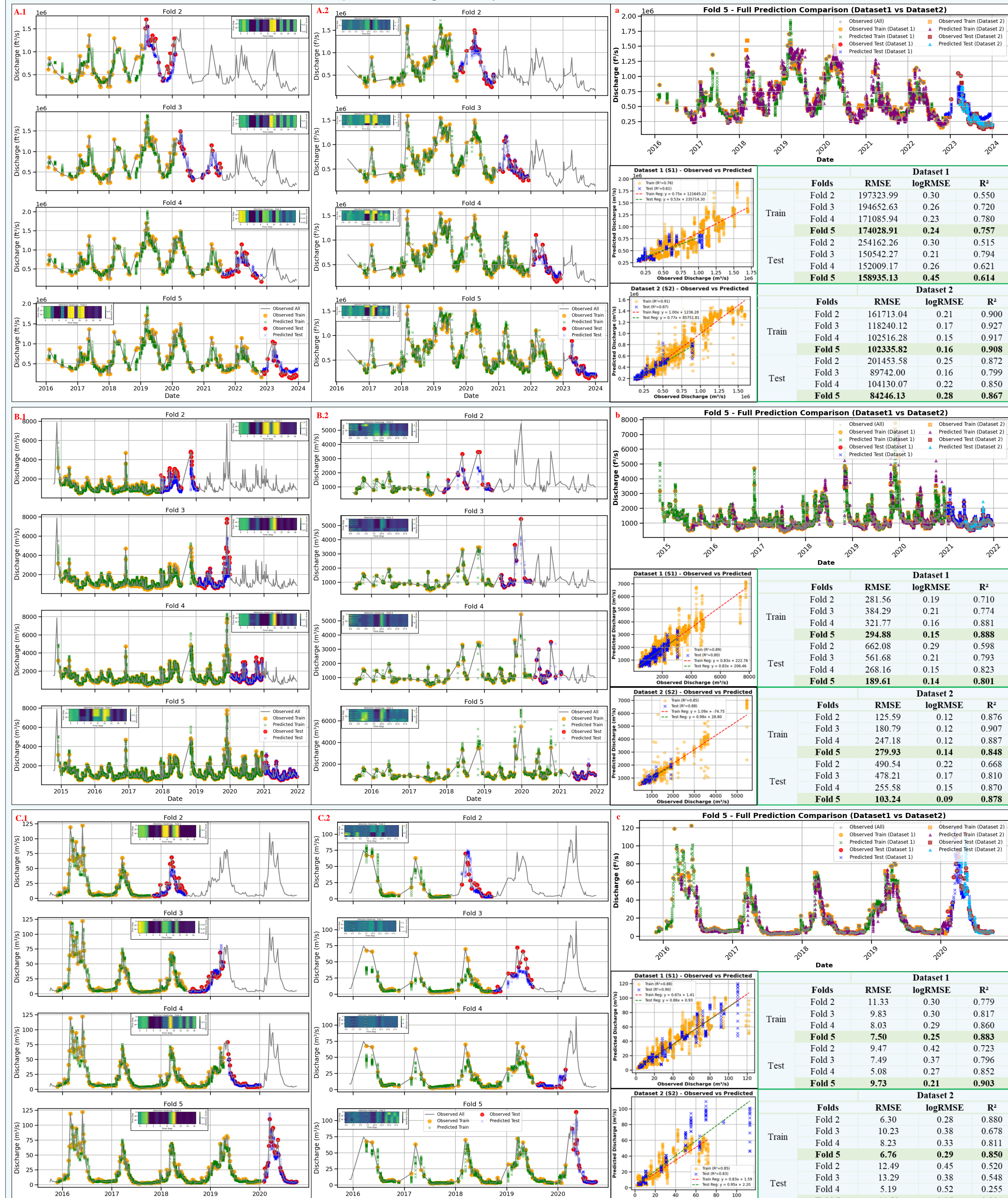


Figure 6: LSTM model results across all regions; (A.1) Memphis Dataset1, (A.2) Memphis Dataset2, (B.1) Pontelagoscuro Dataset1, (B.2) Pontelagoscuro Dataset2, and (C.1) Sogutluhan Dataset1, (C.2) Sogutluhan Dataset2. Time-series predictions across Fold 2 to Fold 5 are shown in the top panels.

**Figure 7:** The LSTM final results of all study sites, including the agreements between observed and estimated discharge for each proposed area; (a) Memphis, (b) Pontelagoscuro, and (c) Sogutluhan.

| Dataset | Folds  | RMSE      | Dataset 1 |                |
|---------|--------|-----------|-----------|----------------|
|         |        |           | logRMSE   | R <sup>2</sup> |
| Train   | Fold 2 | 197233.99 | 0.30      | 0.550          |
|         | Fold 3 | 194653.63 | 0.26      | 0.720          |
|         | Fold 4 | 171085.94 | 0.23      | 0.780          |
|         | Fold 5 | 174028.91 | 0.24      | 0.757          |
|         | Fold 5 | 102335.92 | 0.16      | 0.908          |
| Test    | Fold 2 | 254162.26 | 0.30      | 0.515          |
|         | Fold 3 | 150542.27 | 0.21      | 0.794          |
|         | Fold 4 | 152009.17 | 0.26      | 0.621          |
|         | Fold 5 | 158935.13 | 0.25      | 0.614          |
|         | Fold 5 | 84246.13  | 0.28      | 0.867          |

## TAKEAWAYS & OUTLOOK

- Attention layers improve interpretability by identifying the temporal relevance of input variables across folds.
- The fold-wise transfer learning approach enhances temporal generalization and helps stabilize predictions across unseen sequences.
- Due to LSTM's lookback structure and satellite data frequency limitations, integration with hydrologic models is essential for achieving daily and stable discharge estimates.
- Expand the methodology to basins with diverse climate and topography.
- Combine LSTM with other machine learning or physically-based models to improve generalizability, especially in mountainous or morphologically dynamic areas.
- Integrate hydrologic modeling components to enable daily discharge estimation.
- Operationalize the approach for automated, large-scale application in ungauged or data-scarce basins.

Figure 5: The workflow of step-wise fold transfer for time-aware LSTM model

In contrast, **Fold 5** represents the *final* evaluation stage. Thanks to the cumulative learning transferred from previous folds, the test accuracy in Fold 5 may even exceed the training accuracy, highlighting cumulative knowledge transfer learning, not overfitting similar to Pontelagoscuro region Dataset 2 and Sogutluhan region Dataset 1 evaluation in Figure 6.

Full-sequence river discharge estimation (Fold 5) indicated that both datasets capture discharge dynamic more effectively than the RF Time-split model (Figure 6). Dataset 2 slightly outperformed Dataset 1 in most metrics, particularly for peak flows, indicated by preliminary performance results (Figure 7).